Tellus
SERIES B
CHEMICAL
AND PHYSICAL
METEOROLOGY
PUBLISHED BY THE INTERNATIONAL METEOROLOGICAL INSTITUTE IN STOCKHOLM

Tellus (2010), 62B, 296–313
Printed in Singapore. All rights reserved

TELLUS

Characterizing post-industrial changes in the ocean carbon cycle in an Earth system model

By KATSUMI MATSUMOTO[1]*, KATHY S. TOKOS[1], MEGUMI O. CHIKAMOTO[1†] and ANDY RIDGWELL[2], [1]*Geology and Geophysics, University of Minnesota, MN, USA*; [2]*School of Geographical Sciences, University of Bristol, Bristol, UK*

(Manuscript received 6 July 2009; in final form 5 May 2010)

ABSTRACT

Understanding the oceanic uptake of carbon from the atmosphere is essential for better constraining the global budget, as well as for predicting the air-borne fraction of CO_2 emissions and thus degree of climate change. Gaining this understanding is difficult, because the 'natural' carbon cycle, the part of the global carbon cycle unaltered by CO_2 emissions, also responds to climate change and ocean acidification. Using a global climate model of intermediate complexity, we assess the evolution of the natural carbon cycle over the next few centuries. We find that physical mechanisms, particularly Atlantic meridional overturning circulation and gas solubility, alter the natural carbon cycle the most and lead to a significant reduction in the overall oceanic carbon uptake. Important biological mechanisms include reduced organic carbon export production due to reduced nutrient supply, increased organic carbon production due to higher temperatures and reduced $CaCO_3$ production due to increased ocean acidification. A large ensemble of model experiments indicates that the most important source of uncertainty in ocean uptake projections in the near term future are the upper ocean vertical diffusivity and gas exchange coefficient. By year 2300, the model's climate sensitivity replaces these two and becomes the dominant factor as global warming continues.

1. Introduction

Over the past two centuries since industrialization, fossil fuel burning and land-use changes have significantly altered the chemical composition of the atmosphere. For instance, by the year 2005, the concentration of CO_2 had already reached 379 ppm compared to a pre-industrial value of ∼280 ppm (IPCC, 2007). This is equivalent to an increase of 210 PgC (1 Pg = 10^{15} g), assuming the conversion factor of 1 ppm = 2.123 PgC (Orr et al., 1999). CO_2 is a major greenhouse gas that modulates the radiative balance of the Earth, and this dramatic (∼one-third) increase in CO_2 in the atmosphere is a primary driver of global warming (GW, IPCC, 2007).

The fate of fossil fuel carbon in recent decades is constrained by data on fossil fuel production and measurements of atmospheric composition (Prentice et al., 2001). Various studies have indicated that roughly 30% (about 2 PgC yr^{-1}) of the annual global emissions of CO_2 (about 7 PgC yr^{-1}) is currently being removed from the atmosphere by oceanic uptake. The means by which this is known include global ^{13}C budgets for CO_2 (Quay et al., 1992; Tans et al., 1993; Heimann and Maier-Reimer, 1996; Quay et al., 2003), ocean forward modelling (Sarmiento et al., 2000; Orr et al., 2001; Matsumoto et al., 2004), ocean inverse modelling (Gloor et al., 2001; Gloor et al., 2003; Mikaloff-Fletcher et al., 2006; Gerber et al., 2009), and combined use of atmospheric O_2 and CO_2 measurements (Keeling and Shertz, 1992; Keeling et al., 1996). While these independent methods have their own uncertainties, they consistently indicate that oceans have absorbed approximately 2 PgC yr^{-1} in the past two decades.

The estimation of the cumulative global ocean uptake of anthropogenic CO_2 since pre-industrial times is an entirely different matter and more challenging for two main reasons. First, there has been a lack, until the mid 1990s, of sufficiently precise measurements of dissolved inorganic carbon (DIC) with global coverage. Precise DIC data are necessary, because the anthropogenic signal contained in the total measured DIC concentration is at most only a few percent. This problem has now been addressed largely by the global, multinational efforts of the World Ocean Circulation Experiment (WOCE) and the Joint Global Ocean Flux Study (JGOFS), which have provided the necessary high quality data of temperature, salinity and geochemical tracers, including DIC and chlorofluorocarbons (CFCs, Key et al., 2004; WOCE Data Products Committee, 2002). The second

*Corresponding author.
e-mail: katsumi@umn.edu
†Now at: Japan Agency for Marine-Earth Science and Technology, Kanagawa, Japan.
DOI: 10.1111/j.1600-0889.2010.00461.x

reason is the lack of empirical knowledge of DIC distribution prior to industrialization. Even with perfect knowledge of the global ocean DIC distribution today, the small anthropogenic component must still somehow be separated from the much larger and unknown pre-industrial (background) component of DIC.

The ΔC^* method, introduced by Gruber et al. (1996), provided an effective solution to the second difficulty. Using many data sets and a number of assumptions, the ΔC^* method is able to identify different contributions to the total DIC concentration; the major contributions are from remineralization of particulate organic carbon (POC) and CO_2 solubility. By subtracting these from the total DIC, the method can ultimately isolate the small anthropogenic signal. Despite its complexity, the ΔC^* method has gained credibility with the ocean carbon cycle community, partly because it represents a substantial improvement over previous methods (Brewer, 1978; Chen and Millero, 1979). Today the ΔC^* method is the most widely applied method to estimate changes in ocean carbon content (Gruber, 1998; Sabine et al., 1999; Sabine et al., 2002; Lee et al., 2003), while other methods exist (Goyet et al., 1999; Hall et al., 2002; Touratier and Goyet, 2004). In a global summary of the ΔC^* results, Sabine et al. (2004) estimate a cumulative uptake of anthropogenic CO_2 of 118 ± 19 PgC through 1994, which agrees with an estimate using transit time distributions (Waugh et al., 2006). This represents about 50% of the fossil fuel CO_2 emitted to the atmosphere between 1800 and 1994. They inferred from this, together with the knowledge of CO_2 emissions and accumulation in the atmosphere, that the terrestrial biosphere was a net source of CO_2 to the atmosphere by 39 ± 28 PgC over this period. However, the validity of this very important inference ultimately hinges crucially on the reliability of the ΔC^*-derived estimates.

Because of the unique and central role that it plays in understanding the global carbon cycle response to anthropogenic emissions, the ΔC^* method has been under much scrutiny (Wanninkhof et al., 1999; Coatanoan et al., 2001; Sabine and Feely, 2001; Hall et al., 2004; Matsumoto and Gruber, 2005). As noted by Keeling (2005), one serious weakness of the ΔC^* method stems from the assumption that the 'natural' ocean carbon cycle has not changed since pre-industrial times. (Here, we define as 'natural', the set of carbon cycle mechanisms excluding fossil fuel emissions and land use change—i.e. the elements of the global carbon cycles not *directly* influenced by the emission of CO_2 to the atmosphere and consequential invasion into the ocean.) By design, the ΔC^* method can only estimate the DIC changes that are directly driven by the anthropogenic perturbation of atmospheric CO_2. The method is not designed to detect DIC changes caused by alterations in the natural carbon cycle in the absence of perturbation in atmospheric CO_2. For example, let us consider GW caused by anthropogenic emission of black carbon. Ocean warming would enhance water column stratification and reduce gas solubility, both of which would reduce the oceanic uptake of CO_2 from the atmosphere. This warming would therefore increase atmospheric CO_2 by moving carbon from the ocean to the atmosphere via the *natural* carbon cycle. This increase in atmospheric CO_2 should rightly be considered anthropogenic as Keeling (2005) would argue, because the warming is ultimately anthropogenic. By design however, the ΔC^* method would miss this, because the increased CO_2 in the atmosphere is derived from a perturbation to the natural system (the ocean).

Observations support the notion that the present ocean may not be in steady state and that the natural carbon cycle is changing. The heat content of the world ocean has increased substantially over the last few decades (Levitus et al., 2000). Also, changes in ocean circulation (McPhaden and Zhang, 2002) and a wide-spread decrease in the oxygen content of thermocline waters in several ocean basins (Matear et al., 2000; Pahlow and Riebesell, 2000; Emerson et al., 2001; Andreev and Watanabe, 2002; Keller et al., 2002) have been reported. These observations indicate that the ocean inventory of anthropogenic CO_2 as defined by the ΔC^* method may indeed be an incomplete measure of the *total* change in ocean carbon content (Keeling, 2005), which is ultimately of more significance for the ongoing global climate change debate.

It is thus important to ask how significant the changes to the natural ocean carbon cycle are, both up to the year 1994, the nominal year for the inventory estimate of Sabine et al. (2004) was made, and in the future under GW. A recent discourse, involving a challenge to the ΔC^* estimate (Keeling, 2005) and its response (Sabine and Gruber, 2005), indicates that there is not yet a consensus, and this serves as the main motivation for this study.

This study builds on previous studies that have investigated carbon-climate feedbacks with climate models of various complexity (Sarmiento et al., 1998; Joos et al., 1999; Matear and Hirst, 1999; Bopp et al., 2001; Plattner et al., 2001; Bopp et al., 2005; Crueger et al., 2008; Zickfeld et al., 2008). These studies have all investigated the physical effects of warming on the natural carbon cycle, looking primarily at upper ocean stratification and CO_2 solubility. Many of the same studies have also investigated the biological effects under GW, but the findings are somewhat more ambiguous. A reason may be that they employ biological schemes of various sophistication, ranging from a simple nutrient diagnostic production (Sarmiento et al., 1998) to multiple nutrient, ecosystem dynamics (Bopp et al., 2005). Generally speaking, the simpler schemes allow for more limited and perhaps less realistic biological responses. Nevertheless, it appears the biological impact on the natural carbon cycle can be important, especially when the North Atlantic Deep Water (NADW) formation is weakened, which is almost universally predicted by climate models under GW and which reduces the supply of nutrient rich waters from the deep to the ocean surface.

In this study, we use a climate model of intermediate complexity to assess many of these and new factors that may impact the natural ocean carbon cycle. The new factors include

biotic response to changes in temperature, which may have had a significant role in the natural CO_2 fluctuations over the glacial–interglacial cycles (Matsumoto, 2007), and biotic response to river runoff of nitrate, which apparently increased by factor of two since the pre-industrial period (Green et al., 2004). Following previous studies (Plattner et al., 2001), we carry out a number of sensitivity runs in order to isolate the individual mechanisms. Finally, we present the results of a large model ensemble in order to assess the robustness of our results to the uncertainties in a set of selected parameters.

2. Model description

The global climate-carbon model that we use in this study is MESMO (Matsumoto et al., 2008). The physical model of MESMO is derived from the computationally efficient C-GOLDSTEIN climate model (Edwards and Marsh, 2005) and consists of a three-dimensional dynamical model of the ocean, a two-dimensional dynamic–thermodynamic model of sea ice and energy and moisture balance model of the atmosphere. In one simulation year, there are 500 time steps for the atmosphere and sea-ice (0.73 day/step), and 100 time steps for the physical ocean (3.65 days/step). The ocean model has 16 levels in the vertical with two layers above the biological compensation depth of 100 m water depth. Here, it is implemented on a 36 × 36 equal-area horizontal grid with 10° increments in longitude and uniform in sine of latitude; latitude spacing increases from about 3° at the equator to about 20° at the poles. Ocean dynamics is based on the thermocline or planetary geostrophic equations with the addition of a linear drag term in the horizontal. The resulting 'frictional geostrophic' equations (Edwards et al., 1998) are therefore similar to classical general circulation models with momentum acceleration and advection neglected. The model includes the Gent-McWilliams eddy mixing parametrization according to Griffies (1998) that reduces excessive vertical mixing in coarse gridded models. Unlike C-GOLDSTEIN, the vertical diffusivity in MESMO has an arctangent depth dependence akin to that of Bryan and Lewis (1979), which significantly improves the interior ocean ventilation in MESMO (Matsumoto et al., 2008). The atmospheric model is an energy and moisture balance model following Weaver et al. (2001). The external forcing by shortwave radiation is seasonal, which helps realize reasonable seasonality in marine export production and polar sea ice coverage. Eddy diffusion coefficients of heat and moisture determine the distributions of surface air temperature and humidity.

The marine biogeochemistry model of MESMO is based on BIOGEM (Ridgwell et al., 2007), which in turn is partly based on the Ocean Carbon Cycle Model Intercomparison Project (OCMIP) BIOTIC code (Najjar et al., 2007). The marine biogeochemistry model runs on-line with the physical ocean model, but updating only one in five ocean time steps (i.e. 20 time steps per year, or 18.25 days/step). Modifications have been made in MESMO so that export production occurs in the top 100 m above the compensation depth and is based on Michaelis–Menton nitrate uptake kinetics with further dependences on light, temperature, mixed layer depth (MLD) and biomass (Matsumoto et al., 2008). The production of $CaCO_3$ occurs in waters supersaturated with carbonate ion with respect to mineral calcite and is related to organic carbon production by a ratio. This ratio depends on the degree of supersaturation, so that in lower pH waters, $CaCO_3$ production is reduced and thus organic carbon to $CaCO_3$ export ratio becomes higher (Ridgwell et al., 2007). Particulate organic carbon (POC) and $CaCO_3$ are produced in the top 100 m with rates that depend on temperature. These particles sink through the water column at a fixed speed but are remineralized at rates that depend on temperature. The temperature dependence of production and remineralization approximately follows the heuristic $Q_{10} = 2$ relationship, where the rate doubles for every 10 °C increase.

The version of MESMO used in this study includes two minor modifications to what is documented (Matsumoto et al., 2008): (1) a corrected parametrization of $CaCO_3$ remineralization, which under some conditions erroneously dissolved more $CaCO_3$ than existed; (2) a complete recalculation of global ocean CO_2 chemistry immediately prior to model output. Compared to the previous documentation, these resulted in very small changes to the control model state. Steady state global annual POC export is now 10.5 PgC yr^{-1} (previously 10.6); global annual $CaCO_3$ production is now 1.1 PgC yr^{-1} (previously 0.9) and cumulative oceanic uptake of anthropogenic carbon for the year 1994 without climate change is 122 PgC (previously 118) and with climate change is 116 PgC (none reported previously). As detailed in Matsumoto et al. (2008), the high degree of agreement with the ΔC^* method-estimate of 118 PgC (Sabine et al., 2004), as well as with observations of CFCs, C^{14} and other tracers, makes MESMO one of the better calibrated models available today.

3. Experiment design

Here we present two sets of experiments simulating the post-industrial period, for which we take year 1765 by convention as our start year (although the results would be essentially unchanged taking, e.g. 1750 or 1800), and ending in year 2300—a time sufficiently far in the future to encompass the likely exhausting of conventional fossil fuel reserves. First, thirteen sensitivity experiments were devised to isolate important biotic and abiotic mechanisms that affect the natural carbon cycle (Table 1). The set includes three experiments on how an idealized increase in river runoff of nitrate, alkalinity and carbon impacts the ocean–atmosphere carbon budget. Second, a set of 100 ensemble runs explored the sensitivity of the model results to key parametrizations in air–sea gas exchange, climate sensitivity, temperature dependent metabolic rates and anthropogenic river inputs of selected tracers. As shown in Fig. 1, atmospheric pCO_2

Table 1. Experiment description and oceanic uptake of anthropogenic carbon (PgC)

	Experiments	Carbon uptake 1994	2100	2300	Salient experimental features
1	C or Control	122	443	919	Constant climate control run
2	GW	116	408	786	Global warming (GW) control run
3	C-Abiotic	125	464	967	Physics-only constant climate control run
4	GW-Abiotic	116	410	778	Physics-only GW control run
5	GW-SolT	124	436	848	GW with constant solubility
6	GW-Abiotic-SolT	124	438	838	GW with constant solubility and without biology
7	GW-ConstCaCO3	112	386	715	GW with constant $CaCO_3$ production
8	GW-ProdT	111	388	727	GW with constant temperature as it relates to production
9	GW-ReminT	117	414	810	GW with constant temperature as it relates to remineralization
10	GW-ProdMLD	115	404	773	GW with constant mixed layer depth as it relates to production
11	GW-RiverN	122	422	819	GW with excess river flux of nitrogen
12	GW-RiverA	129	438	866	GW with excess river flux of alkalinity
13	GW-RiverC	115	407	784	GW with excess river flux of carbon

Notes: The control experiment C does not include atmospheric radiative feedback; GW experiment does. Abiotic experiments have no biology. GW-SolT, GW-ProdT, GW-ReminT are the same as GW except that ocean temperatures are maintained at the preindustrial values, as they relate respectively to gas exchange, production and remineralization. GW-ProdMLD is the same as GW except that the MLD as it relates to production only is maintained at the preindustrial levels. GW-Const$CaCO_3$ maintains the preindustrial $CaCO_3$ production and thus ignores the pH dependence. The three GW river experiments introduce excess river run off as described in Section 3. All experiments are forced by the prescribed atmospheric pCO_2 shown in Fig. 1.

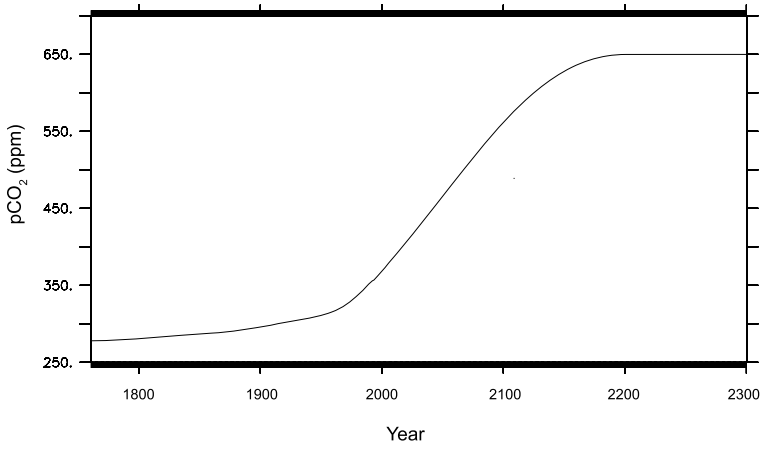

Fig. 1. Atmospheric pCO_2 forcing function, a combination of observations 2005 (Enting et al., 1994; Keeling and Whorf, 2005) and the WRE S650 stabilization scenario (Wigley et al., 1996).

in all experiments is prescribed to follow observations from 1760 to 2005 (Enting et al., 1994; Keeling and Whorf, 2005) and thereafter the WRE S650 stabilization scenario to 2300 (Wigley et al., 1996). In the S650 scenario, atmospheric CO_2 concentrations increase until stabilized at 650 ppm in the year 2200. The scenario is within the range of IPCC SRES scenarios (Nakicenovic et al., 2000) and slightly above the doubling of CO_2 pre-industrial concentrations, which now seems very challenging to meet (Hoffert et al., 1998; Pielke et al., 2008). We chose to prescribe atmospheric pCO_2 in this study instead of using CO_2 emissions as we have done previously (Nusbaumer and Matsumoto, 2008) because we are interested primarily in isolating the CO_2 contributions by individual mechanisms without the complications of having variable CO_2 radiative feedback. Most of our analysis will focus on simulation year 1994, for which anthropogenic carbon estimates of Sabine et al. (2004) are available, and 2100, a future time within a hundred years from now.

In the first set of experiments (Table 1), the constant climate control experiment is forced with prescribed atmospheric pCO_2 without the CO_2 radiative feedback. GW experiments include the CO_2 radiative feedback. Experiments C-Abiotic and GW-Abiotic are identical to the control and GW experiments respectively, except that they are abiotic (i.e. no production and remineralization of POC and $CaCO_3$). These abiotic

experiments are analogous to the ABIOTIC simulations of OCMIP-2 (Orr et al., 1999), where the physical processes were examined in isolation from the biological processes represented in the BIOTIC simulations (Najjar and Orr, 1999). Experiments GW-SolT and GW-Abiotic-SolT are, respectively, identical to the GW and GW-Abiotic experiments, except they maintain the pre-industrial SSTs as they relate to gas exchange only, so that the solubility effect of GW can be isolated. Likewise, experiment GW-Const$CaCO_3$ is a GW experiment with pre-industrial $CaCO_3$ production. Similarly, experiments GW-ProdT and GW-ReminT are GW experiments with pre-industrial ocean temperatures only as they relate to biological production and remineralization rates, respectively. Experiment GW-ProdMLD is a GW experiment with pre-industrial MLDs as they relate to biological production only. The design of the last three experiments allows us to examine how GW affects the natural ocean carbon cycle through biology.

The final three GW experiments in the first set of experiments are GW-RiverN, GW-RiverA and GW-RiverC (Table 1). These investigate the effects of increasing the runoff of excess nitrate, alkalinity and carbon. The input of excess nitrogen can enhance biological production and thus the natural carbon cycle. In a global synthesis, Green et al. (2004) estimate that global runoff flux of nitrogen to the oceans has roughly doubled (40 Tg-N yr^{-1}; Tg = 10^{12} g) since pre-industrial times (21 Tg yr^{-1}). Their basin-by-basin breakdown of the excess 19 Tg yr^{-1} reflects how anthropogenic nitrogen is loaded geographically to the continental landmass. In experiment GW-RiverN, we linearly increase the global flux of excess nitrate (as well as alkalinity associated with it) from zero in year 1765 to 19 Tg yr^{-1} in 2000 and for simplicity continue to linearly increase it to 42 Tg yr^{-1} in 2300. As a point of reference, our prescribed flux is four orders of magnitude smaller than the nitrogen fluxes associated with future denitrification and nitrogen fixation simulated in a model as a result of releasing 5100 PgC or roughly all of known fossil fuels (Schmittner et al., 2008). In GW-RiverN, excess nitrate is introduced to the ocean model domain along the coast, where runoff is expected, following the land surface runoff directions of C-GOLDSTEIN. The excess nitrate flux differs by basin according Green et al. (2004) but is the same within a given basin (i.e. no point sources).

The river input of excess alkalinity can change the natural carbon cycle by increasing the buffer capacity of the ocean. At the same time, the input of carbonate alkalinity derived from continental weathering will also change the anthropogenic carbon cycle, because this is in the form of either carbonate (CO_3^{2-}) or bicarbonate (HCO_3^-) ions which contain carbon. Raymond and Cole (2003) report that alkalinity runoff in the Mississippi watershed, dominated by bicarbonate ions, has increased by roughly 50% in the past 50 yr. It seems likely that alkalinity runoff has increased elsewhere as well, especially in regions of urbanization, which is shown to increase the runoff of solutes including alkalinity (Rose, 2007). However, there is neither basin-by-basin breakdown nor global synthesis for alkalinity that will help guide us in setting up the alkalinity runoff experiments. Therefore, we extrapolate the Mississippi case and simply assume for lack of constraint that the global river flux of alkalinity, estimated to be 2.6×10^{13} mole-eq yr^{-1} during the pre-industrial period (Milliman, 1993), increased linearly by 50% from 1765 to 2000. In GW-RiverA, excess alkalinity is delivered to the ocean as bicarbonate and equally to those coastal grid cells that receive runoff. As with nitrogen, we assume that the linear increase in alkalinity input continues to the end of the simulation in year 2300.

The last river input we examine is carbon, and this comes in the form of POC and dissolved organic carbon (DOC). An estimate for the modern flux of carbon by rivers worldwide is approximately 380 Tg-C yr^{-1} (Meybeck, 1993; Ludwig et al., 1996). This can be broken down into DOC (∼55%) and POC (∼45%); most of the POC is derived from repeated erosion and weathering and considered inert. The modern flux of 380 Tg-C yr^{-1} can be considered to represent the mid 1980s when relevant river water measurements were made, and so it already contains fluxes due to humans in addition to the pre-industrial flux. There is no observational constraint to separate the anthropogenic flux, so we will simply assume as before that the modern flux represents a 50% increase over the pre-industrial and that it continues to increase linearly in the future. In experiment GW-RiverC, excess carbon is delivered to the ocean as DOC and equally to those coastal grid cells that receive runoff. POC is assumed to be relatively refractory in nature and buried in marine sediments.

In all three river experiments, the input flux is obviously highly idealized. Also, the coarse resolution of MESMO makes it difficult to accurately represent the shallow coastal waters. Our aim with in these experiments is thus not necessarily to make realistic predictions, but to assess the potential impact of these factors in comparison to more commonly considered feedbacks (e.g. the temperature–solubility relationship) and within the same Earth system model.

In the second set of experiments, we seek to quantify the robustness of the model response to changes in five key parameters (Table 2) with an ensemble of 100 simulations, each 535 yr long, starting in year 1765 and ending in 2300 just like the GW experiment in Table 1. Two simulations were done for each set of parameters, one with increasing atmospheric CO_2, including radiative feedback, and with constant atmospheric CO_2 forcing. The run with constant forcing gives the correction for model drift, which arises from parameters being changed in year 1765 without prior adjustment. Each 535-yr run took about 1 h. With the available computing resources, the entire ensemble of 200 simulations took just under 1 d. The five parameters are: (1) air–sea gas exchange coefficient; (2) climate sensitivity; (3) degree of temperature dependence of metabolic rates; (4) multiplier of anthropogenic river inputs and (5) the upper ocean vertical diffusivity. These were chosen for the important role that they play in carbon uptake as recognized previously in the case of

Table 2. Ensemble model run description

	Experiment GW	Ensemble range
Parameter		
Gas exchange coefficient (m d^{-1})	0.31	0.20–0.34
Climate sensitivity (°C)	3.5	1.8–4.8
Biotic temperature dependence modifier	1.0	0.5–1.5
River input modifier	1.0	0.5–1.5
Upper ocean vertical diffusivity (10^{-4} m^2 s^{-1})	0.1	0.05–0.15
Oceanic inventory of anthropogenic carbon		
Year 1994	116	105–120
Year 2100	408	380–431
Year 2300	786	727–863

Note: See Section 4.3 for the explanation of the five parameters and their ranges.

(1), (2) and (5) (e.g. Sarmiento et al., 1992) or for novelty in the case of (3) and (4). Our choice of parameters was guided by the focus of this study.

The first key parameter is the gas exchange coefficient, which in MESMO is based on the quadratic dependence on the steady wind speed (Wanninkhof, 1992), although other forms of dependence such as cubic and linear have been suggested. While the quadratic Wanninkhof coefficient remains the de facto standard in existing ocean carbon cycle models, recent reanalysis of bomb ^{14}C inventory in the ocean suggest that it may be too high by 20–33% (Naegler et al., 2006; Sweeney et al., 2007; Muller et al., 2008). We therefore choose a range that encompasses these estimates at the low end and 10% higher than the Wanninkhof value at the high end. Second, the equilibrium climate sensitivity of MESMO, which in the standard configuration is 3.5 °C for CO_2 doubling, is prescribed to encompass the full range of the most recent IPCC assessment (2.1–4.4 °C) (IPCC, 2007). This parameter would account for changes in the physical state of climate including ocean circulation. Third, the degree to which marine production and remineralization rates depend on temperature, now set at the heuristic $Q_{10} = 2$ (doubling for a 10 °C increase), will be allowed to vary by ±50%. Fourth, the river inputs of nitrate, alkalinity and carbon are also allowed to covary by ±50% of the standard input forcing described above, assuming that hydrological changes affect all inputs proportionally. Finally, the upper ocean vertical diffusivity was allowed to vary by ±50% about the control value of 0.1×10^{-4} m^{-2} s^{-1}. The derivation of the arctangent depth profile of vertical diffusivity in MESMO is fully described by Matsumoto et al. (2008) and includes a multi-objective optimization method, a population based algorithm to seek pareto-optimal solutions in the parameter space, and subjective tuning, which explored various arctangent shapes. The vertical diffusivity, particularly in the upper ocean above the arctangent transition, was recognized as the single most important parameter of calibration for MESMO in terms of transient tracer uptake. Our value is consistent with available data-based estimates of this parameter (Gregg, 1989; Polzin et al., 1995), which are too few in number to reveal its true variability in the ocean.

The five parameters take random values within their specified ranges (Table 2), thus sweeping the five-dimensional parameter space uniformly. The range of the ocean carbon uptake by the ensemble thus indicates the uncertainty in the results to the choice of these five important parameters.

4. Results

4.1. Biotic and abiotic responses to pCO_2 increase

In the control run, where CO_2 radiative feedback is turned off, there is no climate change. Oceanic carbon uptake in MESMO increases as atmospheric pCO_2 increases: 122 PgC in 1994, 443 PgC in 2100 and 919 PgC in 2300 (Experiment 1, Table 1). Directly comparing these absolute inventories to previous studies is not straightforward, because the atmospheric CO_2 forcing we have used differs from the various business-as-usual emissions forcings or CO_2 trajectories employed previously. However, on the basis of the reasonable performance of the MESMO model in simulating observed transient tracer inventories such as CO_2 and CFCs (Matsumoto et al., 2008), the future CO_2 predictions should be comparable to other models with comparable degrees of model skill in simulating transient tracers. Model skill can be evaluated using data-based metrics (Matsumoto et al., 2004; Cao et al., 2009).

With no climate change in the control run, POC export in MESMO remains unchanged at 10.5 PgC yr^{-1}. However, $CaCO_3$ export production is reduced as the surface ocean becomes more acidic and less favourable to calcification. By year 2100, the pH of the global surface ocean is reduced by about 0.2, and the global $CaCO_3$ export is reduced by 55% from the pre-industrial 1.1 PgC yr^{-1} with a greater reduction occurring in high latitudes (57%) than in the low latitudes (45%) because of the different Revelle (buffer) factors. All else being equal, the reduced $CaCO_3$ export or carbonate pump would increase the surface ocean alkalinity and thereby enhance the oceanic carbon uptake. This is shown below in experiment GW-Const$CaCO_3$.

In the GW experiment, anthropogenic carbon uptake is reduced compared to the control experiment (Table 1). The reduction is about 5% in 1994 (116 instead of 122 PgC) and becomes larger as GW becomes more significant reaching about 8% in 2100 (408 instead of 443 PgC). These fractional changes in the uptake are comparable to previous studies (Sarmiento et al., 1998; Joos et al., 1999; Matear and Hirst, 1999; Plattner et al., 2001; Crueger et al., 2008). Figure 2 illustrates how the GW

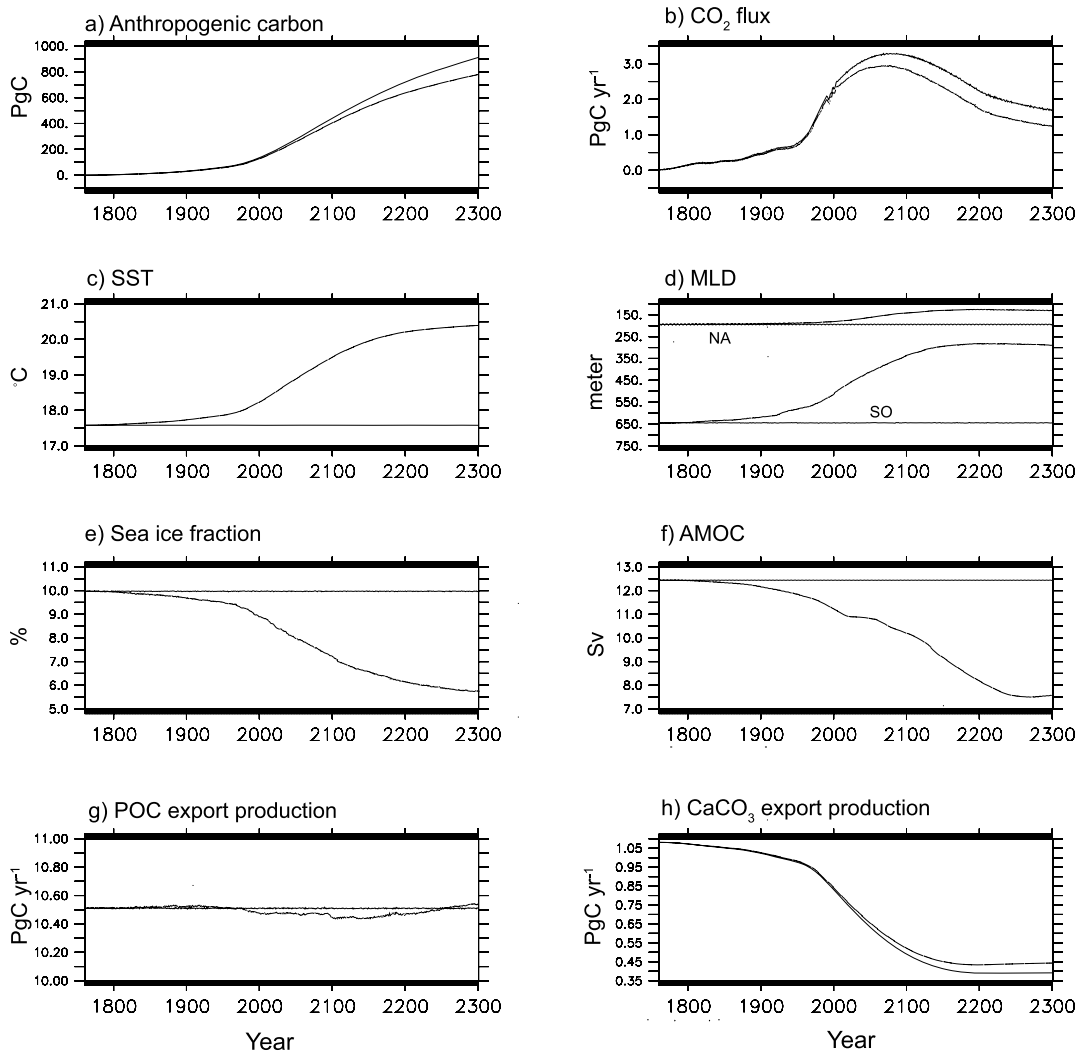

Fig. 2. Time series of global annual mean diagnostics from the control experiment (solid) and GW experiment (dashed): (a) inventory of anthropogenic carbon in the ocean (PgC); (b) atmosphere-to-ocean CO_2 flux (PgC yr^{-1}); (c) sea surface temperature; (d) surface mixed layer depth (m) for the Southern Ocean (SO) and the North Atlantic (NA); (e) sea ice coverage (% world ocean area); (f) Atlantic meridional overturning circulation (Sv); (g) POC export production (PgC yr^{-1}); (h) $CaCO_3$ export production (PgC yr^{-1}).

experiment differs from the control experiment and offers hints as to which are the important mechanisms in explaining the difference. The reduction in the carbon uptake in the GW experiment relative to the control experiment is evident in both the oceanic inventory (Fig. 2a) and annual CO_2 flux (Fig. 2b). The inventory increases monotonically because the global net flux is always from the atmosphere into the ocean. Warming in the upper ocean (Fig. 2c) makes the upper waters more buoyant and stratified, thus shoaling the MLD (Fig. 2d). The shoaling is largest in the Southern Ocean where annual mean MLD was hundreds of meters deep. Warming also causes the polar sea ice to retreat (Fig. 2e) and the Atlantic meridional overturning circulation (MOC) to weaken (Fig. 2f). The overall export of POC is minimally affected (Fig. 2g), although as we argue below there are multiple effects that offset one another to produce relatively constant production. The overall $CaCO_3$ export production declines (Fig. 2h) as noted above, but less so under warming, which lowers the solubility product of calcite, increases the carbonate ion saturation concentration with respect to calcite, and therefore tends to promote calcification. Note in Fig. 2 that the climate has largely stabilized by year 2300 as indicated by SST, MLD, sea ice and MOC, but carbon cycle has not.

The contribution of the physical mechanisms to the total reduction in carbon uptake under GW is given by the difference between the two abiotic experiments GW-Abiotic and C-Abiotic (Table 1). With GW, oceanic carbon uptake is reduced by 7% in year 1994 (116 instead of 125 PgC) and 12% in year 2100 (410 instead of 464 PgC). As identified previously, one of the important physical mechanisms is gas solubility, which is reduced with increasing temperature (Fig. 2c). The solubility effect is given

independently by two sets of experiments: the biotic set GW and GW-SolT; and the abiotic set GW-Abiotic and GW-Abiotic-SolT (Table 1). In both sets, the solubility effect reduced carbon uptake by about 6% in 1994 (116 instead of 124 PgC for both biotic and abiotic) and in 2100 (408 instead of 436 PgC for biotic, 410 instead of 438 PgC for abiotic). The difference between the total physical contribution and solubility contribution essentially gives the contribution of ocean circulation, which reduces carbon uptake by 1% (7% reduction by total physical effects, 6% reduction due to solubility) in 1994 and by 6% (12 and 6% reductions) in 2100. The increasingly larger impact of changes in circulation is consistent with it changing more as GW becomes more severe.

As noted above, the reduction in $CaCO_3$ export with increasing acidity enhances carbon uptake. Comparison of experiments GW and GW-Const$CaCO_3$, which maintains the pre-industrial $CaCO_3$ export throughout the GW, confirms this (Table 1). With declining $CaCO_3$ export, the carbon uptake is increased by about 4% in 1994 (116 instead of 112 PgC) and 6% in 2100 (408 instead of 386 PgC), within the range of model predictions of Ridgwell et al. (2007).

Three ways by which GW can impact the soft tissue pump are illustrated by experiments GW-ProdT, GW-ReminT and GW-ProdMLD (Table 1). The first two experiments control for the fact that organic matter production rates and remineralization rates, respectively, depend on temperature, which has the potential to exert significant influence on atmospheric pCO_2 (Matsumoto, 2007). The GW experiment compared to GW-ProdT shows that warming speeds up production, enhancing the soft tissue pump, and therefore increases carbon uptake by about 5% in 1994 (116 instead of 111 PgC) and 2100 (408 instead of 388 PgC). In contrast, experiment GW-ReminT shows that warming reduces the soft tissue pump by remineralizing POC more quickly and at shallower depths, so that the carbon uptake under GW is lowered by 1% in 1994 (116 instead of 117 PgC) and slightly more in 2100 (408 instead of 414 PgC). Finally, GW can impact the efficiency of the soft tissue pump by altering the MLD, as shown by Sverdrup (1953) in his seminal work on the spring bloom. Increased shoaling of MLD under GW (Fig. 2d) relative to the critical depth increases the export production, so that carbon uptake is higher by about 1% in 1994 (116 instead of 115 PgC) and 2100 (408 instead of 404 PgC).

These warming-driven changes in the oceanic uptake of carbon are not uniform in space. As illustrated for year 2100, the largest change occurs in the Atlantic Ocean for both the biotic experiments (GW-control, Fig. 3a) and abiotic experiments (GW-Abiotic minus C-Abiotic, Fig. 3b). Of the total difference of 35 PgC between experiments GW and control for 2100, 15 PgC is in the Atlantic, followed by 12 PgC in the Pacific and 8 PgC in the Indian. The similarity between the biotic and abiotic experiments indicates that much of this spatial heterogeneity is caused by physical mechanisms. In particular, much of the spatial heterogeneity originates from changes in ocean circulation, because warming and thus the gas solubility effect tends to be rather uniform in space (Fig. 4a). This circulation contribution is obtained by subtracting the solubility effect from the total physical effects in abiotic experiments (Fig. 4b): reduction in carbon uptake by 1% in 1994 and 6% in 2100. Although this difference would include the effect of shrinkage in sea ice (Fig. 2e), this effect is evidently secondary as the changes in the carbon inventory shown in Fig. 4b occur mostly outside the polar regions. In fact, the largest change in DIC is seen in the deep North Atlantic below about 1000 m, whereas the change in DIC above 1000 m is comparable between that the Atlantic and the Pacific (Fig. 5).

Some of the warming-induced changes in the carbon uptake driven by biology also show distinct spatial patterns (Fig. 6), although the biologically driven changes are generally smaller in amplitude than physically driven changes. The reduction of $CaCO_3$ export production is most pronounced in the North Atlantic, where carbon uptake is enhanced (Fig. 6a). The temperature effects on the production rates (Fig. 6b) and remineralization rates (Fig. 6c) are most evident in the Southern Ocean. It is not that warming is strongest in the Southern Ocean. Rather these results indicate that temperature, instead of other factors like nutrients and light, was limiting production to a greater extent in the Southern Ocean in the control run. Finally, shoaling of MLD occurs everywhere but most pronounced in the Southern Ocean (Fig. 2d), and therefore MLD-induced increase in POC export and carbon uptake are most pronounced in the Southern Ocean (Fig. 6d; amplitude is rather small to be detected with the common color scale of Fig. 6).

4.2. Response to River Inputs

Figure 7 shows how oceanic uptake of carbon is impacted by the prescribed river inputs of nitrate, alkalinity and carbon. In each panel, the solid line is the carbon uptake when river inputs are prescribed under GW. Two reference lines provide context to the three river experiments. The first reference, which serves as the lower bound and indicated by dashed line, is the uptake in the GW experiment in Table 1; it has no river input. Therefore, the difference between the solid and dashed lines indicates how the inputs have altered the carbon uptake. The second reference, which serves as the upper bound and indicated by dotted line, is defined differently in each case.

In the riverine nitrate experiment (GW-RiverN), the upper bound is a theoretical maximum uptake driven by the soft tissue pump. It is the carbon uptake which would be realized if the entire riverine nitrate were converted to export production. Thus, it would be 7.3 times (C/N = 117/16) the nitrate input, according to the C:N elemental stoichiometry of biological uptake. However, as explained in Appendix S1, this theoretical value is achievable only in a simple ocean box model under a special condition. In a dynamical biogeochemical model like

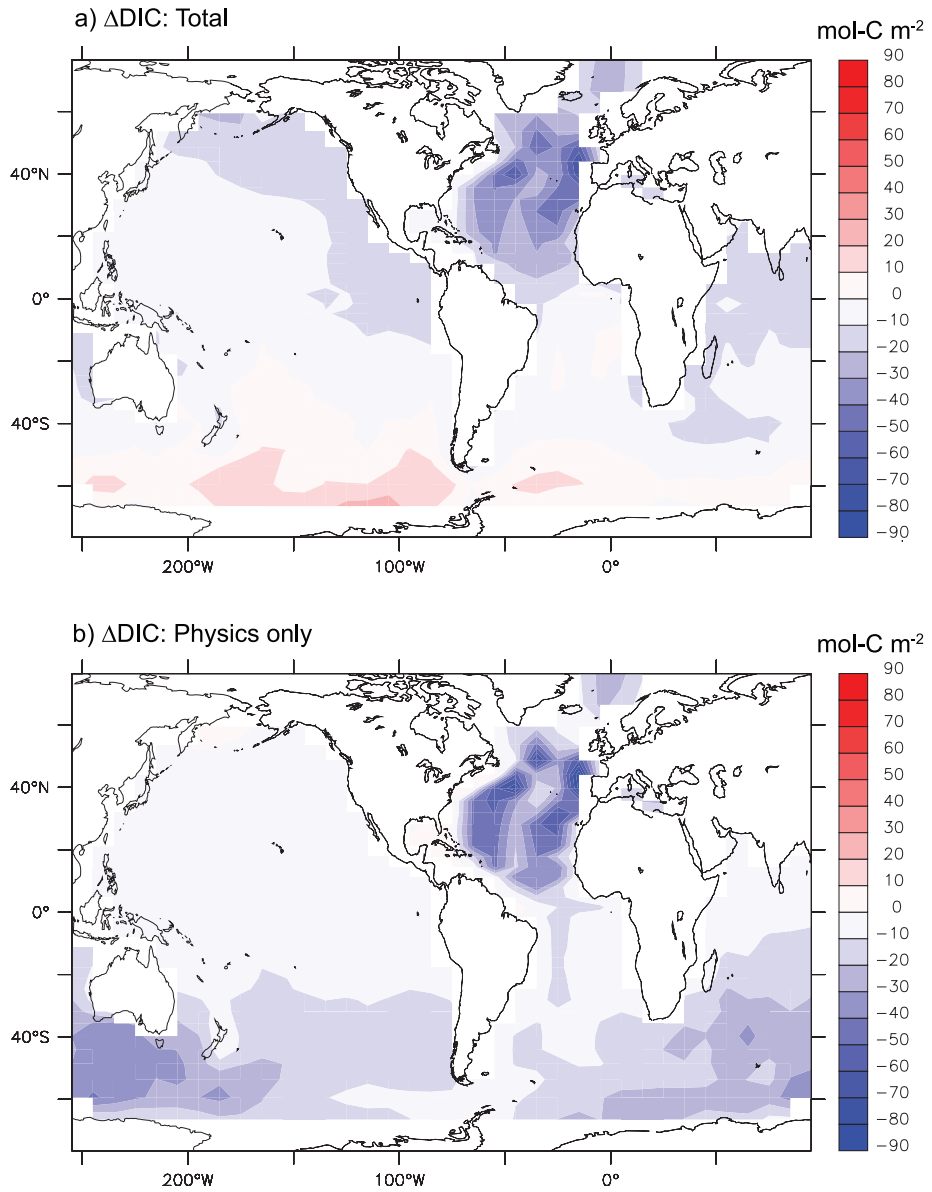

Fig. 3. Changes in the 2100 column inventory of DIC (mole-C m^{-2}): (a) 'total' including biotic and abiotic factors from experiments GW-C; (b) 'total physics' from experiments GW-Abiotic minus C-Abiotic.

MESMO, even when the entire riverine nitrate is removed from the surface waters, the actual carbon uptake is less than the theoretical maximum. The first reason for this is that the addition of nitrate, an anion, removes alkalinity in the same molar ratio. So the surface water pCO_2 rises, all else being the same. The second reason is that some of the excess surface nitrate is removed by circulation. In an imaginary case where a very large amount of nitrate is added, circulation acting on the high concentration gradient will remove nitrate even in the absence of biology. In GW-RiverN, the fact that the uptake in the model (solid line) is approximately half way between the lower bound (dashed line) and the upper bound (dotted line) indicates that a significant fraction of the riverine nitrate ultimately led to new production that enhanced carbon uptake from the atmosphere (Fig. 7a).

In the riverine alkalinity experiment (GW-RiverA), the addition of alkalinity in the form of bicarbonate increases DIC in the same molar ratio as alkalinity. So we use the cumulative DIC addition as the upper bound reference. In Fig. 7b, the oceanic carbon inventory for GW-RiverA (solid line) is nearly the same as the upper bound reference (dotted line), indicating that all the carbon that was added remained in the ocean without enhancing the uptake. This makes sense because the carbonate ion concentration is approximately equal to the difference between

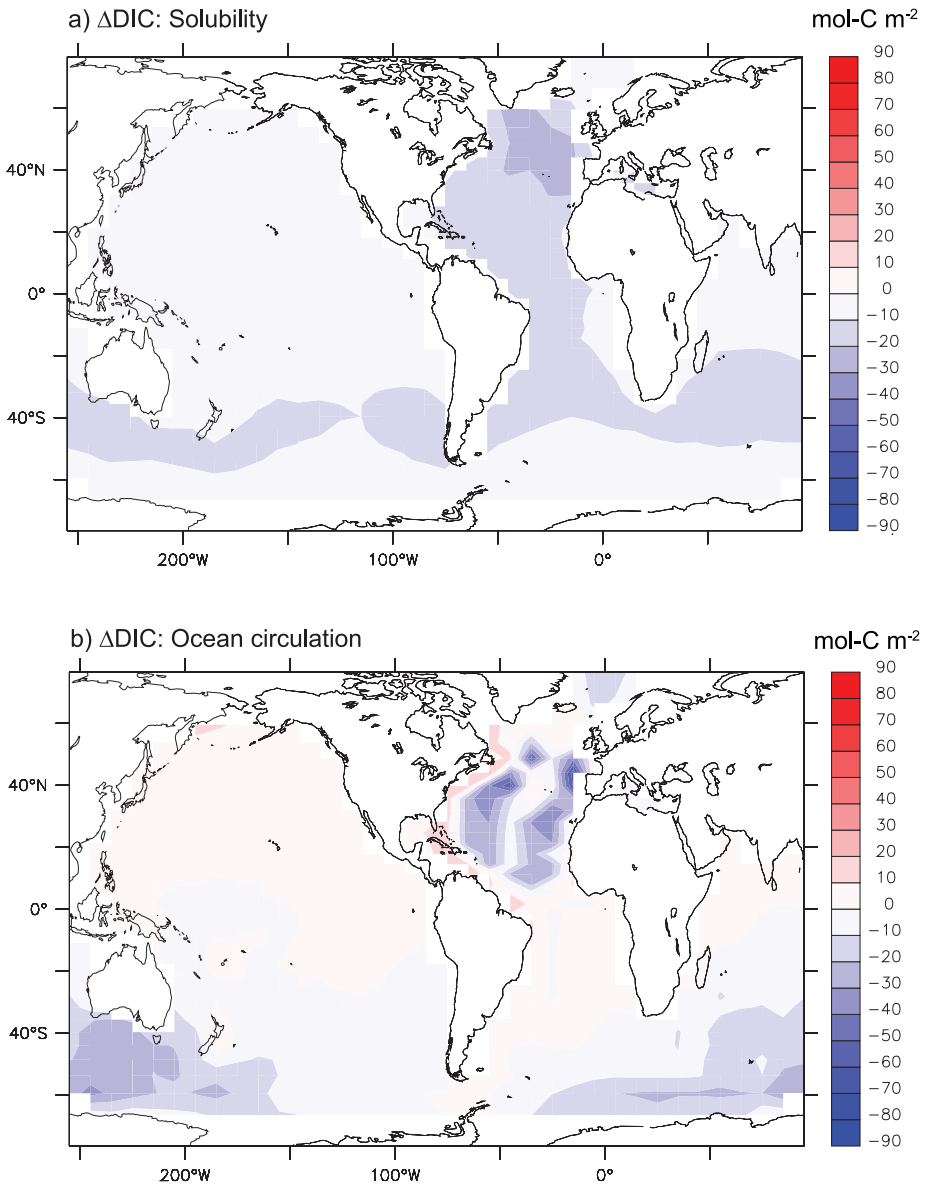

Fig. 4. Changes in the 2100 column inventory of DIC (mole-C m^{-2}) due to physical factors: (a) solubility from experiments GW minus GW-SolT (or from the equivalent abiotic experiments); (b) Difference between total physics and solubility attributed to 'ocean circulation' from three experiments: GW-Abiotic minus C-Abiotic minus GW-Abiotic-SolT.

alkalinity and DIC and inversely related to pCO_2. Therefore, the addition of alkalinity in the form of bicarbonate does not significantly impact the surface water pCO_2 and hence net air–sea CO_2 flux. If alkalinity were added in the form of carbonate ion instead, surface water pCO_2 would be have been reduced and carbon uptake enhanced.

In the riverine carbon experiment (GW-RiverC), carbon was introduced in the form of DOC. Therefore, a convenient upper bound reference is again the cumulative amount introduced. That would be realized in the model if the entire DOC added remained in the ocean. If so, the likely form of carbon would be DIC as DOC is decomposed and repartitioned between the atmosphere and the ocean. As seen in Fig. 7c though, the uptake in GW-RiverC (solid line) is nearly identical to the base GW experiment (dashed solid, hidden). Because the water column DOC inventory stays essentially unchanged (not shown), this indicates that most of the carbon input did not stay in the ocean after DOC decomposition. Another way to put it in these prescribed pCO_2 runs is that DOC decomposition raised the surface water pCO_2 and reduced the net transfer of carbon from the atmosphere by about the same amount that entered via rivers.

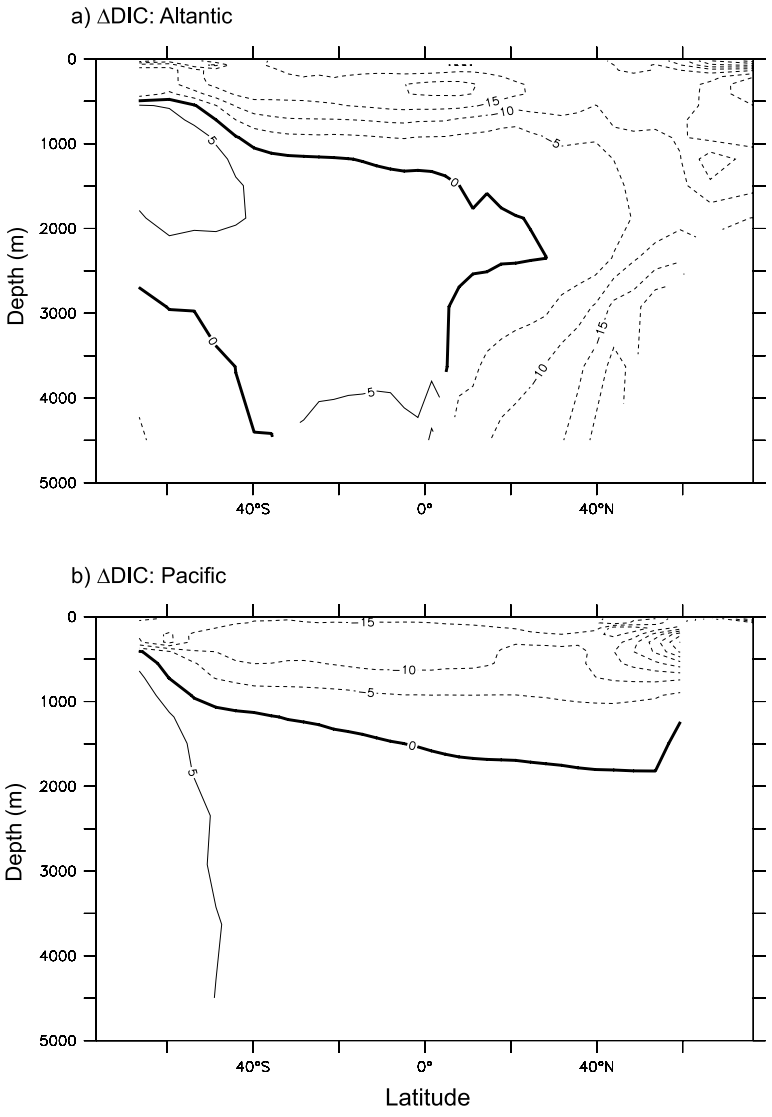

Fig. 5. Changes in the 2100 zonally averaged DIC concentrations (μmole-C kg^{-1}) under global warming (experiments GW-C) in the Atlantic Ocean (a) and Pacific Ocean (b).

Although not shown, the sum of the carbon uptakes from the three individual river input experiments is nearly the same as the uptake from a single experiment that included all three river inputs. The combined effect of any non-linearity in this regard is therefore minimal.

4.3. Ensemble model runs

The net CO_2 uptake by the ocean predicted in the ensemble ($n = 100$) is 113 $\pm$ 6 PgC (2σ) in 1994, 406 $\pm$ 22 PgC in 2100 and 794 $\pm$ 64 PgC in 2300 (Fig. 8). The general trend is a function of the prescribed atmospheric pCO_2, and the range of uncertainty in model projections, which becomes larger with time, is a function of the model's sensitivity to the combined effects of the variation of five parameters that take random values within specified ranges (Table 2). We compare these effects by comparing years 1994 and 2300; resulting trends are similar for year 2100, although smaller in magnitude. Of those considered here, the most important parameter contributing to the uncertainty in carbon uptake is identified by plotting the oceanic uptake against the range of each parameter (Fig. 9) and calculating a linear least squares regression to calculate the amount of variance that may be prescribed to that parameter. For 1994, the uptake correlates most significantly with the upper ocean vertical diffusivity (Fig. 9i) with the highest r^2 value (0.53), followed by the gas transfer coefficient ($r^2 = 0.35$, Fig. 9a) and climate sensitivity ($r^2 = 0.11$, Fig. 9c). This means that the choice of the upper ocean vertical diffusivity and gas exchange coefficient is most important in determining the 1994 uptake: the higher the coefficients, the greater the carbon uptake. It is generally understood that the transfer of a tracer from the atmosphere to the

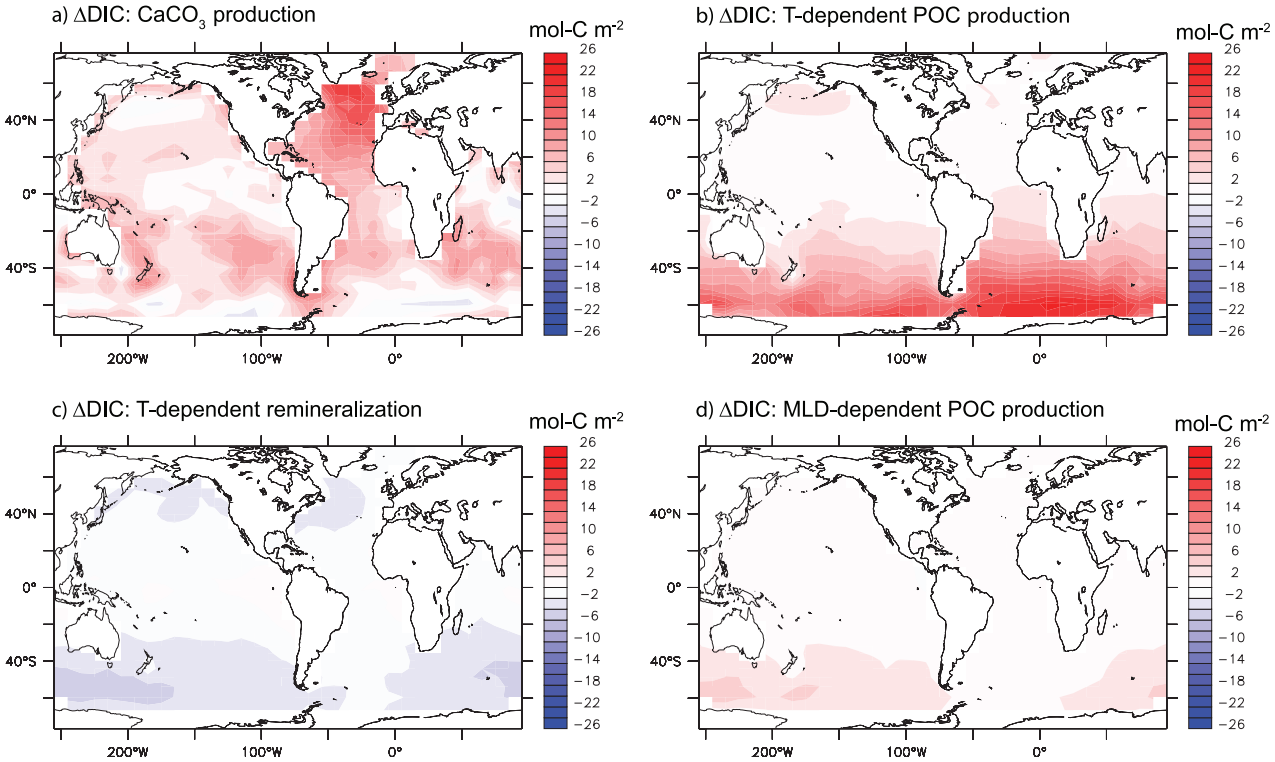

Fig. 6. Changes in the 2100 column inventory of DIC (mole-C m^{-2}) due to biological factors: (a) $CaCO_3$ production, from experiments GW minus GW-Const$CaCO_3$; (b) temperature dependent POC production, from experiments GW minus GW-ProdT; (c) temperature dependent POC and $CaCO_3$ remineralization, from experiments GW minus GW-ReminT and (d) MLD dependent POC production, from experiments GW minus GW-ProdMLD.

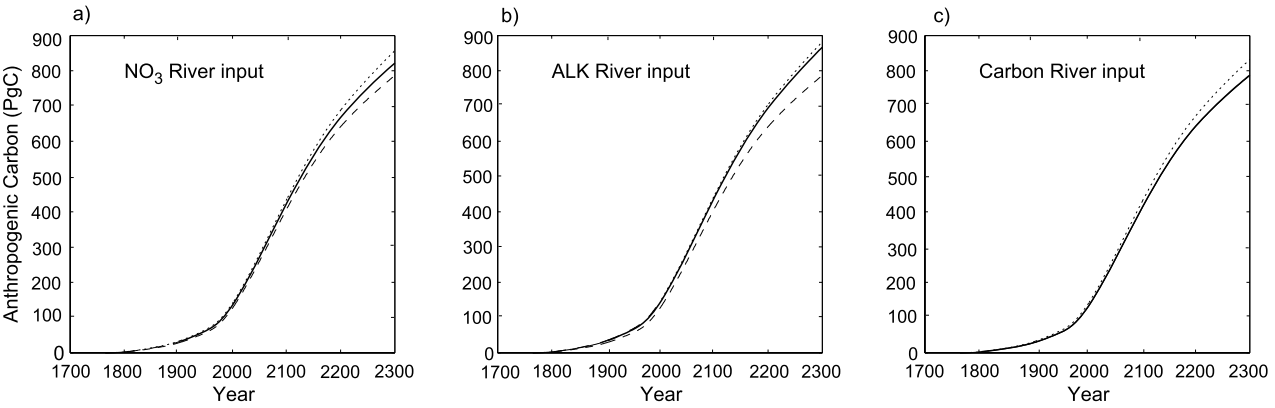

Fig. 7. Carbon uptake (PgC) under global warming with prescribed anthropogenic river inputs of: (a) nitrate; (b) alkalinity and (c) carbon. Dashed line is the reference uptake from experiment GW (Table 1). Dotted line is the upper bound reference if all the input in carbon equivalent remained in the ocean. Solid line shows the model-predicted uptake with river inputs.

ocean is rate-limited by these processes and that for a relatively fast equilibrating gas like CO_2 (unlike $^{14}CO_2$ for example), the more limiting step is the upper ocean mixing (Sarmiento et al., 1992). Our results are thus consistent with this notion. Note that the ensemble mean of 113 PgC in 1994 is not the same as 116 PgC (Experiment GW, Table 1), because the range is not centred about the default gas exchange coefficient (Table 2).

In the future and by 2300, the choice of the upper ocean vertical diffusivity and gas exchange coefficient becomes less important (Figs 9b and j), while the model's climate sensitivity becomes the most important determinant of oceanic carbon uptake ($r^2 = 0.74$, Fig. 9d). This is consistent with the fact that the uncertainty in the carbon uptake increases with time, as GW becomes more severe. By comparison, the degree to which

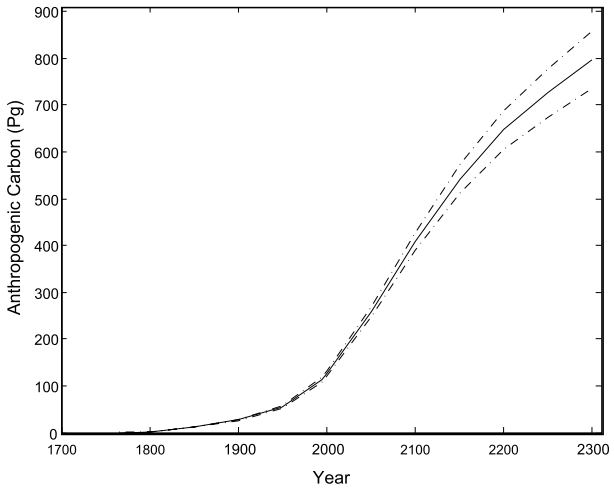

Fig. 8. Carbon uptake in the ensemble of model runs. The ensemble mean is the middle solid line and the dash–dotted lines indicate 2σ. The uptake is 113 ± 6 PgC in 1994, 406 ± 22 PgC in 2100 and 794 ± 64 PgC in 2300. See Table 2 for ensemble run description.

metabolic rates change with temperature and how much river inputs deviates from the standard input forcing are insignificant for both times (Figs 9e–h). Note that this does not mean that, for example, the temperature dependence of metabolic rate is unimportant in oceanic uptake of anthropogenic carbon. As discussed in the next section, it is important. The point here is that the parametrization of that dependence, given its uncertainty, is not as important as how gas exchange and climate sensitivity are parametrized.

Another important point concerns the overall estimated uncertainty in carbon uptake in our ensemble. This reflects not only the allowed range of values of the five parameters, but also the assumed structure and parametrization choices of MESMO which has previously been calibrated against observations of physical and biogeochemical properties (Matsumoto et al., 2008). As a result, the ensemble may not provide a very broad range of global ocean circulation states, but a relatively narrow one already constrained by observations. That the estimated uncertainty across the ensemble is apparently smaller than previous data-based estimates of CO_2 inventory does mean that the model ensemble presented here is in any sense more certain than other estimates, but simply that given the structure of MESMO, the range of possible CO_2 inventories is narrower. This is valuable, as by further refining the independent observationally estimated CO_2 inventory, any statistical incompatibility arising between model and data-based estimates would tell us that one or more assumptions and/or parametrizations in MESMO are fundamentally incorrect. The purpose of this study in any case is to help refine the data-based estimates of the inventory (e.g. ΔC^*) by quantifying the potential contribution made by the natural carbon cycle rather than to supplant data-based methods.

5. Discussion

Increasing atmospheric pCO_2 is the dominant cause of the overall oceanic uptake of anthropogenic carbon. This is clear in our study from the fact that the CO_2 flux into the ocean is greatest (Fig. 2b), when atmospheric pCO_2 is rising most rapidly (Fig. 1) and therefore the pCO_2 gradient across the air–sea interface, which drives the flux, is the largest. However, changes to the global climate and ocean dynamics due to GW in MESMO, such as reduced polar sea ice, shoaling of the MLD and slowdown of the Atlantic MOC (Fig. 2), impact the oceanic uptake of carbon as well. To understand the implication of these impacts on a human timescale, we compare the year 2100 to the base year 1994. We find that when CO_2 radiative feedback is activated in the GW experiment, the uptake is reduced by 5% in 1994 and 8% in 2100 compared to the control experiment (Table 1). The magnitude of these responses is well within the range of previous studies (e.g. Sarmiento and Le Quere, 1996; Sarmiento et al., 1998; Joos et al., 1999; Matear and Hirst, 1999; Plattner et al., 2001; Crueger et al., 2008; Zickfeld et al., 2008).

Taking these results at face value implies that the ΔC^*-estimated uptake of 118 ± 19 PgC for 1994 by Sabine et al. (2004) should be reduced by 5%, because the ΔC^* method does not account for GW. The 5% offset would be attributed to changes in the natural carbon cycle as defined above.

Figure 10 summarizes the breakdown of the 5% reduction for 1994 and 8% for 2100 into smaller components of the natural carbon cycle that we have explicitly quantified. As noted previously (Sarmiento and Le Quere, 1996; Sarmiento et al., 1998; Joos et al., 1999; Matear and Hirst, 1999; Plattner et al., 2001; Crueger et al., 2008), physical mechanisms, essentially the solubility and ocean circulation effects, contribute very significantly to the overall reduction in carbon uptake under GW. The solubility effect is global in extent (Fig. 4a) and consistently important as it reduces the carbon uptake by 6% in 1994 and 2100 (Fig. 10). The physical circulation effect, which we obtain by subtracting the solubility effect from the total GW effect in the abiotic experiments, evidently becomes increasingly important with time (1% reduction in 1994, 6% reduction in 2100). The change in the predominance between the solubility effect and the circulation effect is consistent with the finding that the solubility effect is most responsible for the reduction in the carbon uptake unless the Atlantic MOC collapses (Joos et al., 1999; Plattner et al., 2001), although in our study the MOC weakens but does not collapse entirely (Fig. 2f).

The importance of the Atlantic MOC in this study is clearly evident in the similarity in the North Atlantic between the total change in the column inventory of anthropogenic carbon (Fig. 3a) and the change attributed only to circulation (Fig. 4b). That this change in the column inventory is due to changes in the deep ocean rather than the upper ocean is illustrated in Fig. 5. Recently, Crueger et al. (2008) also show that column inventory of anthropogenic carbon is significantly lower in the North

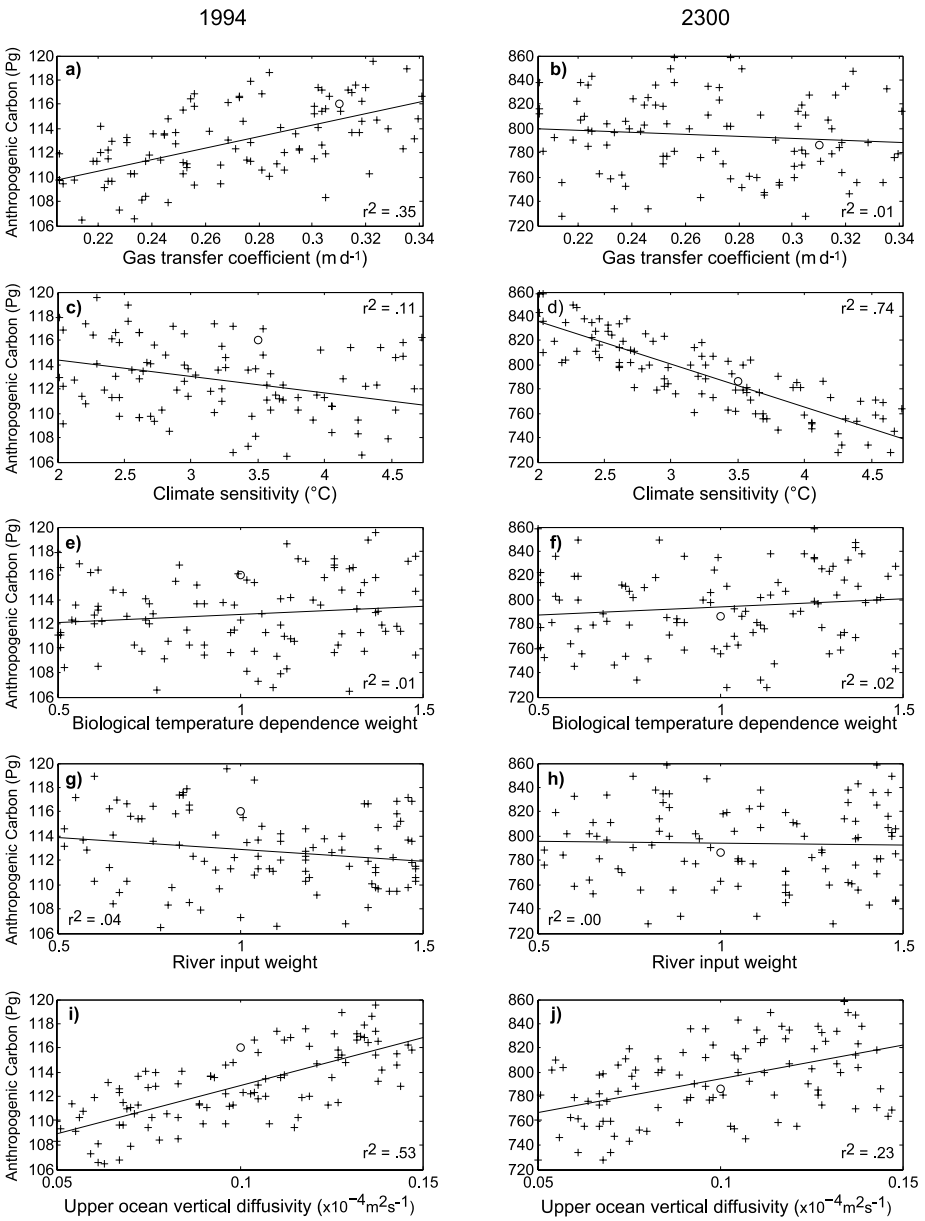

Fig. 9. Correlation between ocean carbon uptake (PgC) in the ensemble of model runs and five key parameters for 1994 (left-hand column) and 2300 (right-hand column). The parameters take random values within specified ranges (Table 2). The correlation coefficient is r, and r^2 indicates the variance explained. Circles represent the reference experiment, GW.

Atlantic in a GW simulation than in their control simulation. They infer therefore that some change in the Atlantic MOC drove this change. With our abiotic experiments, we can point to the physical aspect of the Atlantic MOC as the main cause.

Figure 10 shows that the biological mechanisms are also important, although taken together their contribution to the overall reduction in oceanic carbon uptake is not as significant as the physical mechanisms. The two quantitatively significant terms are the reduction in $CaCO_3$ export due to ocean acidification and the increase in POC export due to warming. They both enhance oceanic uptake of carbon and are mechanisms that have previously not been investigated. In their careful studies, Joos et al. (1999) and Plattner et al. (2001) have looked into how $CaCO_3$ export may be impacted by GW. We extend their work by examining the dependence of $CaCO_3$ production on pH. By considering the effect of the carbonate chemistry on $CaCO_3$ production, we show that the pH dependence is important (Fig. 2h) and the lack of this dependence likely caused previous studies to attribute a relatively modest significance to $CaCO_3$ export. However, the response of pelagic calcifiers to ocean

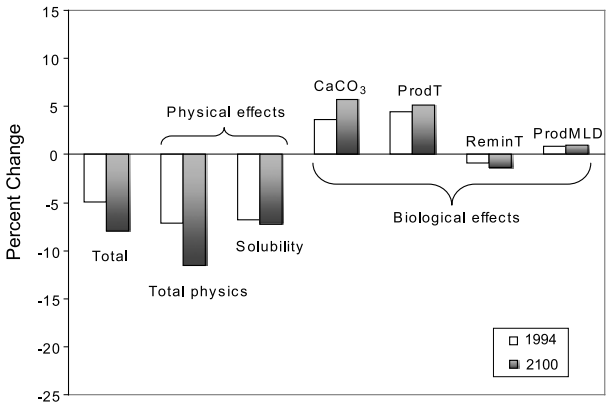

Fig. 10. Percent change in the carbon uptake under the S650 scenario, including global warming, in 1994 and 2100. These were obtained explicitly as the difference between experiment GW (or its abiotic equivalent GW-Abiotic) and sensitivity experiments in Table 1: "Total" from GW-C; 'Total physics' from GW-Abiotic minus C-Abiotic; 'Solubility' from GW minus GW-SolT (or from equivalent abiotic experiments); '$CaCO_3$' from GW minus GW-Const$CaCO_3$; 'ProdT' from GW minus GW-ProdT; ReminT from GW minus GW-ReminT; ProdMLD from GW minus GW-ProdMLD. See Table 1 for values and Section 3 for explanation.

acidification and thus future changes in global carbonate export have yet to be sufficiently well understood (Ridgwell et al., 2009). The other two new biological mechanisms we quantified are changes to the soft tissue pump by MLD shoaling and warming-induced remineralization. These act in the opposite directions and are minor in amplitude (Fig. 10).

The one other important biological mechanism concerns nutrient supply and the effect that ocean circulation has on biology. Specifically, an important implication of stratification and MOC slow down is a reduction in the vertical transport of nutrients to the surface layer from below. This would reduce the soft tissue pump and thus the carbon uptake. In fact, it has even been suggested as the single most important mechanism in reducing the carbon uptake under GW (Zickfeld et al., 2008), while other studies still consider the physical mechanisms to be the most important (Sarmiento and Le Quere, 1996; Sarmiento et al., 1998; Joos et al., 1999; Matear and Hirst, 1999; Plattner et al., 2001; Crueger et al., 2008). As in previous studies, we can estimate the magnitude of the nutrient supply effect by assuming that the individual contributions to the total change are linear. In this study, we obtain this missing contribution by subtracting the total physical effects and the four biological effects ($CaCO_3$, ProdT, ReminT and ProdMLD), all explicitly obtained (Fig. 10), from the total change. Using the data shown in Fig. 10, the nutrient supply effect would thus be -7% for both 1994 ($-5-(-7+4+5-1\,1+1)$) and 2100 ($-8-(-12+6+5-1\,1+1)$). It is indeed negative (i.e. reduces carbon uptake) as we expected. At face value, the nutrient supply effect is as important as the other individual effects identified in Fig. 10. However, in terms of the overall global POC export, the negative nutrient supply effect is largely diminished by the positive temperature-dependent production effect, so the overall change in the soft tissue pump is minimal (Fig. 2g). This would again make the physical effects the dominant cause of the change in the natural carbon cycle.

The river input experiments showed to first order that alkalinity input leads to the greatest carbon uptake or retention on a molar basis. Essentially, alkalinity, which is assumed to enter the ocean in the form of bicarbonate (Raymond and Cole, 2003), just stays in the ocean. In contrast, the input of carbon in the form of DOC does not lead to substantial increase in the oceanic carbon inventory, because it is remineralized and escapes to the atmosphere. This suggests that river input of carbon may in fact add to the increase in atmospheric pCO_2 due to direct emissions. Nitrate input has an intermediate impact. The expected full impact of the soft tissue pump is not realized in part because the addition of nitrate, an anion, essentially removes alkalinity in the equivalent molar basis.

The ensemble of model runs, which explored the parameter space defined by the five key parameters in Table 2, indicates that these river inputs are not important in the post-industrial carbon cycle at the global scale. They do not add substantially to the uncertainty in projections of anthropogenic carbon in the ocean (Figs 9g and h). This is consistent with recent studies that also find very small impacts of increased river inputs on the ocean carbon cycle (Chuck et al., 2005; Cotrim da Cunha et al., 2007). Similarly, the temperature dependence of marine metabolic rates is not important (Figs 9e and f). The three most important parameters are the upper ocean vertical diffusivity, gas exchange coefficient and model's climate sensitivity. In 1994, the upper ocean mixing, which replaces tracer-saturated surface waters with unsaturated interior waters, and gas exchange coefficient, which controls the air–sea CO_2 flux, are the most important of the five parameters (Sarmiento et al., 1992). However, over time climate sensitivity, which controls the severity of the CO_2-induced GW, becomes increasingly more important. A lesson from the ensemble runs is thus that the projection of future carbon uptake by the ocean would benefit perhaps most significantly from the improved understanding of the sensitivity of the global climate to increased greenhouse gases rather than from a more accurate determination of upper ocean mixing, air–sea gas exchange kinetics, marine biology or river inputs.

We note finally that it is beyond the scope of this study and the capabilities of MESMO to examine changes in the natural ocean carbon cycle caused by internal oscillations of the climate system such as regime shifts in ENSO and ocean ventilation related to the Arctic Oscillation.

6. Conclusions

Using a global climate model of intermediate complexity, we isolated and quantified many of the important mechanisms that are responsible for the oceanic uptake of natural and anthropogenic

carbon in the post-industrial period. We find that warming-induced changes in ocean physics, which include slow down of the Atlantic MOC and reduced gas solubility, are the dominant mechanisms that reduce the natural carbon uptake. Important biological mechanisms are reduction in POC production due to reduced nutrient supply, increase in POC production due to warming and reduction in $CaCO_3$ production due to acidification. There is significant uncertainty in how much river fluxes of nitrate, alkalinity and carbon have increased over the post-industrial period, but their contribution to the overall increase in the ocean carbon inventory seems limited compared to other factors. The three most important factors that contribute to the uncertainty in model projections of carbon uptake are the upper ocean vertical diffusivity and gas exchange coefficient, which becomes less important with time as GW becomes more severe, and the model's climate sensitivity, which determines the severity of GW and becomes increasingly important.

7. Acknowledgments

This research was supported by the Office of Science (BER), U.S. Department of Energy grant (DE-FG02-06ER64216) and the University of Minnesota McKnight Land-Grant Professorship. AR acknowledges the Royal Society in the form of a University Research Fellowship and NERC grant NE/F002408/1.

References

Andreev, A. and Watanabe, S. 2002. Temporal changes in dissolved oxygen of the intermediate water in the subarctic North Pacific. *Geophys. Res. Lett.* **29**(14), doi:10.1029/2002GL015021.

Bopp, L., Aumont, O., Cadule, P., Alvain, S. and Gehlen, M. 2005. Response of diatoms distribution to global warming and potential implications: a global model study. *Geophys. Res. Lett.* **32**(19), doi:10.1029/2005GL023653.

Bopp, L., Monfray, P., Aumont, O., Dufresne, J.-L., Treut, H.L. and co-authors. 2001. Potential impact of climate change on marine export production. *Global Biogeochem. Cycles* **15**(1), 81–99.

Brewer, P.G. 1978. Direct observation of the oceanic CO_2 increase. *Geophys. Res. Lett.* **5**, 997–1000.

Bryan, K. and Lewis, L.J. 1979. A water mass model of the world ocean. *J. Geophys. Res.* **84**, 2503–2518.

Cao, L., Eby, M., Ridgwell, A., Caldeira, K., Archer, D. and co-authors. 2009. The role of ocean transport in the uptake of anthropogenic CO_2. *Biogeosciences* **6**, 375–390.

Chen, C.-T. and Millero, F.J. 1979. Gradual increase of oceanic CO_2. *Nature* **277**, 205–206.

Chuck, A., Tyrrell, T., Totterdell, I.J. and Holligan, P.M. 2005. The oceanic response to carbon emissions over the next century: investigation using three ocean carbon cycle models. *Tellus Ser. B-Chem. Phys. Meteorol.* **57**(1), 70–86.

Coatanoan, C., Goyet, C., Gruber, N., Sabine, C.L. and Warner, M. 2001. Comparison of two approaches to quantify anthropogenic CO_2 in the ocean: results from the northern Indian Ocean. *Global Biogeochem. Cycles* **15**, 11–25.

Cotrim da Cunha, L., Buitenhuis, E.T., Le Quere, C., Giraud, X. and Ludwig, W. 2007. Potential impact of changes in river nutrient supply of global ocean biogeochemistry. *Global Biogeochem. Cycle* **21**(GB4007), doi:10.1029/2006GB002718.

Crueger, T., Roeckner, E., Raddatz, T., Schnur, R. and Wetzel, P. 2008. Ocean dynamics determine the response of oceanic CO_2 uptake to climate change. *Clim. Dyn.* **31**(2–3), 151–168.

Edwards, N.R. and Marsh, R. 2005. Uncertainties due to transport-parameter sensitivity in an efficient 3-D ocean-climate model. *Clim. Dyn.* **24**, 415–433.

Edwards, N.R., Willmott, A.J. and Killworth, P.D. 1998. On the role of topography and wind stress on the stability of the thermohaline circulation. *J. Phys. Oceanogr.* **28**, 756–778.

Emerson, S., Mecking, S. and Abell, J. 2001. The biological pump in the subtropical North Pacific Ocean: nutrient sources, Redfield ratios, and recent changes. *Global Biogeochem. Cycles* **15**(3), 535–554.

Enting, I.G., Wigley, T.M.L. and Heimann, M. 1994. Future emissions and concentrations of carbon dioxide: key ocean/atmosphere/land analyses. Technical report 31, CSIRO. Division of Atmospheric Research, p. 127.

Gerber, M., Joos, F., Vazquez-Rodriguez, M., Touratier, F. and Goyet, C. 2009. Regional air-sea fluxes of anthropogenic carbon inferred with an Ensemble Kalman Filter. *Global Biogeochem. Cycles* **23**(GB1013), doi:10.1029/2008GB003247.

Gloor, M., Gruber, N., Hughes, T.M.C. and Sarmiento, J.L. 2001. Estimating net air-sea fluxes from ocean bulk data: methodology and applications to the heat cycle. *Global Biogeochem. Cycles* **15**(4), 767–782.

Gloor, M., Gruber, N., Sarmiento, J., Sabine, C., Feeley, R.A. and co-authors. 2003. A first estimate of present and preindustrial air-sea CO_2 flux patterns based on ocean interior carbon measurements and models. *Geophys. Res. Lett.*. **30**(1), doi:10.1029/2002GL015594.

Goyet, C., Coatanoan, C., Eischield, G., Amaoka, T., Okunda, K. and co-authors. 1999. Spatial variation of total CO_2 and total alkalinity in the northern Indian Ocean: a novel approach for the quantification of anthropogenic CO_2 in seawater. *J. Mar. Res.* **57**, 135–163.

Green, P.A., Vorosmarty, C.J., Meybeck, M., Galloway, J., Peterson, B.J. and co-authors 2004. Pre-industrial and contemporary fluxes of nitrogen through rivers: a global assessment based on typology. *Biogeochemistry* **68**, 71–105.

Gregg, M.C. 1989. Scaling turbulent dissipation in the thermocline. *J. Geophys. Res.* **94**(C7), 9686–9698.

Griffies, S.M. 1998. The Gent-McWilliams skew flux. *J. Phys. Oceanogr.* **28**(5), 831–841.

Gruber, N. 1998. Anthropogenic CO_2 in the Atlantic Ocean. *Global Biogeochem. Cycles* **12**(1), 165–192.

Gruber, N., Sarmiento, J.L. and Stocker, T.F. 1996. An improved method for detecting anthropogenic CO_2 in the oceans. *Global Biogeochem. Cycles* **10**(4), 809–837.

Hall, T.M., Haine, T.W.N. and Waugh, D.W. 2002. Inferring the concentration of anthropogenic carbon in the ocean from tracers. *Global Biogeochem. Cycles* **16**(4), doi:10.1029/2001GB001835.

Hall, T.M., Waugh, D.W., Haine, T.W.N., Robbins, P.E. and Khatiwala, S. 2004. Estimates of anthropogenic carbon in the Indian Ocean with allowance for mixing and time-varying air-sea CO_2 disequilibrium. *Global Biogeochem. Cycles* **18**(GB1031), doi:10.1029/2003GB002120.

Heimann, M. and Maier-Reimer, E., 1996. On the relations between the oceanic uptake of CO_2 and its carbon isotopes. *Global Biogeochem. Cycles* **10**(1), 89–110.

Hoffert, M.I., Caldeira, K., Jain, A., Haites, E., Harvey, L.D. and co-authors. 1998. Energy implications of future stabilization of atmospheric CO_2 content. *Nature*. **395**, 881–884.

IPCC, 2007. Climate Change 2007: the Physical Science Basis. *Contribution of Working Group I to the Fourth Assessment Report of the Intergovernmental Panel on Climate Change*. Cambridge University Press, Cambridge, 996.

Joos, F., Plattner, G.-K., Stocker, T.F., Marchal, O. and Schmittner, A. 1999. Global warming and marine carbon cycle feedbacks on future atmospheric CO_2. *Science* **284**, 464–467.

Keeling, C.D. and Whorf, T.P. 2005. Atmospheric CO_2 records from sites in the SIO air sampling network, Trends: a Compendium of Data on Global Change. CDIAC, Oak Ridge National Laboratory, Oak Ridge, Tennessee.

Keeling, R.F. 2005. Comment on "The ocean sink for anthropogenic CO_2". *Science* **308**, 1743c.

Keeling, R.F., Piper, S.C. and Heimann, M. 1996. Global and hemispheric CO_2 sinks deduced from changes in atmospheric O_2 concentration. *Nature* **381**, 218–221.

Keeling, R.F. and Shertz, S.R. 1992. Seasonal and interannual variations in atmospheric oxygen and implications for the global carbon cycle. *Nature* **358**, 723–727.

Keller, K., Slater, R.D., Bender, M. and Key, R.M. 2002. Possible biological or physical explanations for decadal scale trends in North Pacific nutrient concentrations and oxygen utilization. *Deep-Sea Res. Part II—Topical Stud. Oceanogr.* **49**(1–3), 345–362.

Key, R., Kozyr, A., Sabine, C., Lee, K., Wannikhof, R. and co-authors. 2004. A global ocean carbon climatology: results from GLODAP. *Global Biogeochem. Cycles* **18**(GB4031), doi:10.1029/2004GB002247.

Lee, K., Choi, S.-D., Park, G.-H., Wanninkhof, R, Peng, T.-H. and co-authors. 2003. An updated anthropogenic CO_2 inventory in the Atlantic Ocean. *Global Biogeochem. Cycles* **17**(4), doi:10.1029/2003GB002067.

Levitus, S., Antonov, J.I., Boyer, T.P. and Stephens, C. 2000. Warming of the world ocean. *Science* **287**, 2225–2229.

Ludwig, W., Probst, J.L. and Kempe, S. 1996. Predicting the oceanic input of organic carbon by contential erosion. *Global Biogeochem. Cycles* **10**(1), 23–42.

Matear, R., Hirst, A.C. and McNeil, B.I. 2000. Changes in dissolved oxygen in the Southern Ocean with climate change. *Geochem., Geophys., Geosyst.*, **1**, doi:2000GC000086.

Matear, R.J. and Hirst, A.C. 1999. Climate change feedback on the future oceanic CO_2 uptake. *Tellus* **51B**(3), 722–733.

Matsumoto, K., 2007. Biology-mediated temperature control on atmospheric pCO_2 and ocean biogeochemistry. *Geophys. Res. Lett.* **34**(L20605), doi:10.1029/2007GL031301.

Matsumoto, K. and Gruber, N. 2005. How accurate is the estimation of anthropogenic carbon in the ocean? An evaluation of the ΔC^* method. *Global Biogeochem. Cycles* **19**(GB3014), doi:10.1029/2004GB002397.

Matsumoto, K., Sarmiento, J.L., Key, R.M., Aumont, O., Bullister, J.L. and co-authors. 2004. Evaluation of ocean carbon cycle models with data-based metrics. *Geophys. Res. Lett.* **31**(L07303), doi:10.1029/2003GL018970.

Matsumoto, K., Tokos, K., Price, A.R. and Cox, S. 2008. First description of the Minnesota earth system model for ocean biogeochemistry (MESMO 1.0). *Geoscient. Model Dev.* **1**, 1–15.

McPhaden, M.J. and Zhang, D.X. 2002. Slowdown of the meridional overturning circulation in the upper Pacific Ocean. *Nature* **415**(6872), 603–608.

Meybeck, M. 1993. C, N, P, and S in rivers: from sources to global inputs. In: *Interactions of C, N, P and S in Biogeochemical Cycles and Global Change* (eds R. Wollast, F. Mackenzie and L. Chou). Springer-Verlag, Berlin, 163–193.

Mikaloff-Fletcher, S.E., Gruber, N., Jacobson, A., Doney, S., Dutkiewcz, S. and co-authors. 2006. Inverse estimates of anthropogenic CO_2 uptake, transport, and storage by the ocean. *Global Biogeochem. Cycles* **20**(GB2002), doi:10.1029/2005GB002530.

Milliman, J.D. 1993. Production and accumulation of calcium carbonate in the ocean: budget of a nonsteady state. *Global Biogeochem. Cycle*. **7**(4), 927–957.

Muller, S.A., Joos, F., Plattner, G.K., Edwards, N.R. and Stocker, T. 2008. Modelled natural and excess radiocarbon—sensitivities to the gas exchange formulation and ocean transport strength. *Global Biogeochem. Cycles* **22**(GB3011), doi:10.1029/2007GB003065.

Naegler, T., Ciais, P., Rodgers, K. and Levin, I. 2006. Excess radiocarbon constraints on air-sea gas exchange and the uptake of CO2 by hte oceans. *Geophys. Res. Lett.* **33**(L11802), doi:10.1029/2005GL025408.

Najjar, R.G., Jin, X., Louanchi, F., Aumont, O., Caldeira, K. and co-authors. 2007. Impact of circulation on export production, dissolved organic matter and dissolved oxygen in the ocean: results from OCMIP-2. *Global Biogeochem. Cycle*, **21**(GB3007), doi:10.1029/2006GB002857.

Najjar, R.G. and Orr, J.C. 1999. *Biotic-HOW TO*. Internal OCMIP Report, LSCE/CEA Saclay, Gif-sur-Yvette, France.

Nakicenovic, N., Davidson, O., Davis, G., Grubler, A., Kram, T. and co-authors. 2000. *Special Report on Emissions Scenarios (SRES)*, Cambridge University Press, Cambridge.

Nusbaumer, J. and Matsumoto, K. 2008. Climate and carbon cycle changes under the overshoot scenario. *Global Planet. Change*. **62**, 164–172.

Orr, J., Najjar, R., Sabine, C. and Joos, F. 1999. *Abiotic-HOWTO*. Internal OCMIP Report, LSCE/CEA Saclay, Gif-sur-Yvette, France.

Orr, J.C., Maier-Reimer, E., Mikolajewicz, U., Monfray, P., Sarmiento, J.L. and co-authors. 2001. Estimates of anthropogenic carbon uptake from four three-dimensional global ocean models. *Global Biogeochem. Cycles* **15**(1), 43–60.

Pahlow, M. and Riebesell, U. 2000. Temporal trends in deep ocean Redfield ratios. *Science*. **287**(5454), 831–833.

Pielke, R.J., Wigley, T. and Green, C. 2008. Dangerous assumptions. *Nature* **452**, 531–532.

Plattner, G.-K., Joos, F., Stocker, T. and Marchal, O. 2001. Feedback mechanisms and sensitivities of ocean carbon uptake under global warming. *Tellus*. **53B**, 564–592.

Polzin, K.L., Toole, J. and Schmidt, R.W. 1995. Finscale parameterizations of turbulent dissapation. *J. Phys. Oceanogr.* **25**(March), 306–328.

Prentice I.C. et al., 2001. The carbon cycle and atmospheric carbon dioxide. In: *Climate Change 2001 – The Scientific Basis: Contribution of Working Group I to the Third Assessment Report of the*

Intergovernmental Panel on Climate Change. (eds J.T. Houghton et al.,) Cambridge University Press, Cambridge.

Quay, P., Sonnerup, R., Westby, T., Stutsman, J. and McNichol, A. 2003. Changes in the $^{13}C/^{12}C$ of dissolved inorganic carbon in the ocean as a tracer of anthropogenic CO_2 uptake. *Global Biogeochem. Cycles*. **17**(1), 1004, doi:10.1029/2001GB001817.

Quay, P.D., Tilbrook, B. and Wong, C.S. 1992. Oceanic uptake of fossil fuel CO_2: carbon-13 evidence. *Science*. **256**, 74–79.

Raymond, P.A. and Cole, J. 2003. Increase in the export of alkalinity from North America's largest river. *Nature*. **301**, 88–91.

Ridgwell, A., Schmidt, D. N., Turley, C., Brownlee, C., Maldonado, M. T. and co-authors. 2009. From laboratory manipulations to Earth system models: scaling calcification impacts of ocean acidification. *Biogeosciences.* **6**, 2611–2623.

Ridgwell, A., Hargreaves, J.C., Edwards, N.R., Annan, J.D., Lenton, T.M. and co-authors. 2007. Marine geochemical data assimilation in an efficient earth system model of global biogeochemical cycling. *Biogeosciences*. **4**, 87–104.

Rose, S. 2007. The effects of urbanization on the hydrochemistry of base flow within the Chattahoochee River Basin (Georgia, USA). *J. Hydrol.*. **341**(1–2), 42–54.

Sabine, C. and Gruber, N. 2005. Response to comment on "The ocean sink for anthropogenic CO_2". *Science* **308**, 1743d.

Sabine, C.L., Feeley, R.A., Gruber, N., Key, R.M., Lee, K. and co-authors. 2004. The oceanic sink for anthropogenic CO_2. *Science* **305**, 367–371.

Sabine, C.L., Feeley, R.A., Key, R.M., Bullister, J.L., Millero, F.J. and co-authors. 2002. Distribution of anthropogenic CO_2 in the Pacific Ocean. *Global Biogeochem. Cycles*. **16**(4), doi:10.1029/2001GB001639.

Sabine, C.L. and Feely, R.A. 2001. Comparison of recent Indian Ocean anthropogenic CO_2 estimates with historical approach. *Global Biogeochem. Cycles* **15**, 31–42.

Sabine, C.L., Key, R.M., Johnson, K.M., Millero, F.J., Poisson, A. and co-authors. 1999. Anthropogenic CO_2 inventory of the Indian Ocean. *Global Biogeochem. Cycles*. **13**(1), 179–198.

Sarmiento, J.L., Hughes, T.M.C., Stouffer, R.J. and Manabe, S. 1998. Simulated response of the ocean carbon cycle to anthropogenic climate warming. *Nature* **393**, 245–249.

Sarmiento, J.L. and Le Quere, C. 1996. Oceanic carbon dioxide uptake in a model of century-scale global warming. *Science* **274**, 1346–1350.

Sarmiento, J.L., Monfray, P., Maier-Reimer, E., Aumont, O., Murnane, R. and co-authors. 2000. Sea-air CO2 fluxes and carbon transport: a comparison of three ocean general circulation models. *Global Biogeochem. Cycles* **14**(4), 1267–1281.

Sarmiento, J.L., Orr, J.C. and Siegenthaler, U. 1992. A perturbation simulation of CO_2 uptake in an ocean general circulation model. *J. Geophys. Res.* **97**(C3), 3621–3646.

Schmittner, A., Oschlies, A., Matthews, H.D. and Galbraith, E.D. 2008. Future changes in climate, ocean circulation, ecosystems, and biogeochemical cycling simulated for a business-as-usual CO_2 emission scenario until year 4000 AD. *Global Biogeochem. Cycle* **22**(GB1013), doi:10.1029/2007GB002953.

Sverdrup, H.U. 1953. On conditions for the vernal blooming of phytoplankton. *J. Conseil Permanent Int. pour l'Exploration de la Mer* **18**, 287–295.

Sweeney, C., Gloor, M., Jacobson, A., Key, R., McKinley, G. and co-authors. 2007. Constraining global air-sea gas exchange for CO_2 with recent bomb ^{14}C measurements. *Global Biogeochem. Cycle*. **21**(GB2015), doi:10.1029/2006GB002784.

Tans, P.P., Berry, J.A. and Keeling, R.F. 1993. Oceanic $^{13}C/^{12}C$ observations: a new window on ocean CO_2 uptake. *Global Biogeochem. Cycles* **7**(2), 353–368.

Touratier, F. and Goyet, C. 2004. Applying the new TrOCA approach to assess the distribution of anthropogenic CO_2 in the Atlantic Ocean. *J. Mar. Syst.* **46**(1–4), 181–197.

Wanninkhof, R. 1992. Relationship between wind speed and gas exchange over the ocean. *J. Geophys. Res.* **97**(C5), 7373–7383.

Wanninkhof, R., Doney, S.C., Peng, T.H., Bullister, J.L., Lee, K. and co-authors. 1999. Comparison of methods to determine the anthropogenic CO_2 invasion into the Atlantic Ocean. *Tellus*. **51B**(2), 511–530.

Waugh, D.W., Hall, T.M., McNeil, B.I., Key, R. and Matear, R. 2006. Anthropogenic CO_2 in the oceans estimated using transit time distribution. *Tellus* **58B**, 376–389.

Weaver, A., Eby, M., Wiebe, E.C., Bitz, C.M., Duffy, P.B. and co-authors. 2001. The UVic earth system climate model: model description, climatology, and applications to past, present and future climates. *Atmos.-Ocean*. **39**, 1713–1724.

Wigley, T.M., Richels, R. and Edmonds, J.A. 1996. Economic and environmental choices in the stabilizationof atmospheric CO_2 concentrations. *Nature* **379**, 240–243.

WOCE Data Products Committee. 2002. WOCE Global Data, Version 3.0. 180/02, WOCE International Project Office, Southampton, UK.

Zickfeld, K., Eby, M. and Weaver, A.J. 2008. Carbon-cycle feedbacks of changes in the Atlantic meridional overturning circulation under future atmospheric CO_2. *Global Biogeochemical Cycles* **22**(GB3024), doi:10.1029/2007GB003118.

Supporting Information

Additional supporting information may be found in the online version of this article:

Appendix S1. Fate of riverine nitrate and ocean carbon uptake.

Please note: Wiley-Blackwell are not responsible for the content or functionality of any supporting materials supplied by the authors. Any queries (other than missing material) should be directed to the corresponding author for the article.